

# Evidence of Fermi bubbles around M31

M. S. Pshirkov<sup>1,2,3\*</sup>, V. V. Vasiliev<sup>4†</sup>, K. A. Postnov<sup>1,5\*‡</sup>,

<sup>1</sup>*Sternberg Astronomical Institute, Lomonosov Moscow State University, Universitetsky prospekt 13, 119992, Moscow, Russia*

<sup>2</sup>*Institute for Nuclear Research of the Russian Academy of Sciences, 117312, Moscow, Russia*

<sup>3</sup>*Pushchino Radio Astronomy Observatory, 142290 Pushchino, Russia*

<sup>4</sup>*IMPRS Max Planck Institute for Astronomy, D-69117, Heidelberg, Germany*

<sup>5</sup>*Faculty of Physics, Lomonosov Moscow State University, 117234, Moscow, Russia*

## ABSTRACT

Gamma-ray haloes can exist around galaxies due to the interaction of escaping galactic cosmic rays with the surrounding gas. We have searched for such a halo around the nearby giant spiral Andromeda galaxy M31 using almost 7 years of Fermi LAT data at energies above 300 MeV. The presence of a diffuse gamma-ray halo with total photon flux  $2.6 \pm 0.6 \times 10^{-9} \text{ cm}^{-2} \text{ s}^{-1}$ , corresponding to a luminosity (0.3–100 GeV) of  $(3.2 \pm 0.6) \times 10^{38} \text{ erg s}^{-1}$  (for a distance of 780 kpc) was found at a  $5.3\sigma$  confidence level. The halo form does not correspond to the extended baryonic HI disc of M31, as would be expected in hadronic production of gamma photons from cosmic ray interaction, nor it is spherically symmetric, as could be in the case of dark matter annihilation. The best-fit halo template corresponds to two 6–7.5 kpc bubbles symmetrically located perpendicular to the M31 galactic disc, similar to the ‘Fermi bubbles’ found around the Milky Way centre, which suggests the past activity of the central supermassive black hole or a star-formation burst in M31.

**Key words:** gamma rays: galaxies, galaxies: individual:M31, ISM: magnetic fields, cosmic rays

## 1 INTRODUCTION

Extended baryonic haloes around spiral galaxies can exist due to gas inflow from their neighbourhood (White & Rees 1978; Fukugita & Peebles 2006). When falling towards the galaxy, this gas can be heated up to virial temperatures  $10^6 - 10^7$  K, producing huge reservoirs of hot gas (coronae). There are several observational manifestations of these coronae: soft diffuse X-ray emission extending up to several ten kpc from the central galaxy (Li et al. 2008), absorption in O VII line (Wang et al. 2005; Bregman & Lloyd-Davies 2007), distortions in the shape of gas clouds (Westmeier et al. 2005) and stripping of gas in the satellite galaxies by the ram-pressure of the halo gas (Blitz & Robishaw 2000), see (Putman et al. 2012) and references therein for a review. Such a hot halo around the Milky Way is established by several different methods (Miller & Bregman 2013).

The Milky Way and other disc galaxies can also be immersed into extended cosmic-ray (CR) halos (De Paolis et al. 1999; Feldmann et al. 2013). It is well known that the Milky Way is not a perfect calorimeter for proton CRs: they rather quickly, on time scales of 10–20

Myr, escape from dense regions of the Galaxy, losing only minor part of their energy in interactions with the interstellar medium (Strong et al. 2007, 2010). However, if strong enough magnetic fields exist far away from central regions of the Galaxy, these CRs would not escape to the intergalactic space, but would be instead retained in the magnetized Galactic halo for a considerable time. Magnetic fields 10–100 times as weak as the Galactic ones  $\mathcal{O}(\mu\text{G})$  could be sufficient to contain these CRs for the cosmological time. Wandering CRs would interact with tenuous ( $\sim 10^{-4} \text{ cm}^{-3}$ ) hot plasma producing gamma-rays via pionic channel. Estimates show that the gamma-ray luminosity of such a halo could be around  $10^{39} \text{ erg s}^{-1}$  at energies above 100 MeV (Feldmann et al. 2013). The size and shape of the halo cannot be firmly established and depend crucially on the propagation properties of CRs. The halo ‘half-light’ radius is estimated to be 20–40 kpc (Feldmann et al. 2013). At smaller scales ( $\sim 10$  kpc), the gamma-ray halo can be non-uniform as evidenced by the ‘Fermi bubbles’ (FB) in the Galaxy (Su et al. 2010; Ackermann et al. 2014).

The contribution of the CR halo around our Galaxy to the isotropic gamma-ray background can be as high as 10%, and it is difficult to disentangle it from the truly extragalactic component. However, such halos can be searched for around other spiral galaxies. The most natural target is the halo around the nearby M31 (Andromeda) galaxy. With the

\* E-mail: pshirkov@sai.msu.ru

† E-mail: vasilyev@mpia.de

‡ E-mail: pk@sai.msu.ru

expected angular size of several degrees and a gamma-ray luminosity of  $\sim 10^{39}$  erg s $^{-1}$ , such a halo could be detected by the Fermi LAT even from the Earth-M31 distance of  $> 700$  kpc. The presence of a hot gas around M31, which is essential for the gamma-ray emission from the CR halo, was recently demonstrated by the discovery of certain absorption features in UV-spectrum of quasars projected on the sky close to the galaxy (Rao et al. 2013; Lehner et al. 2015) and distortions in the observed CMB spectrum in the vicinity of M31 due to interference from the halo gas (De Paolis et al. 2014).

## 2 DATA AND DATA ANALYSIS

In our analysis we have used 81 months of Fermi LAT data collected since 2008 Aug 04 (MET = 239557417 s) until 2015 Jul 06 (MET = 457860004 s). We have selected events that belong to the "SOURCE" class in order to have a sufficient number of events without loss in their quality. The PASS8\_V2 reconstruction and v10r0p5 $^1$  version of the Fermi science tools was used. As the expected signal is weak and diffuse, we have selected events with energies larger than 300 MeV, because at lower energies the Fermi LAT point spread function (PSF) quickly deteriorates. Usual event quality cut, namely that the zenith angle should be less than  $100^\circ$  (which is sufficient at these energies) has been imposed.

Smaller PSF allowed us to use smaller region of interest (RoI) as well – we took a circle of 10 degrees around the centre of the M31 galaxy ( $\alpha_{J2000} = 10.6846^\circ$ ,  $\delta_{J2000} = 41.2692^\circ$ ). The data were analysed using the binned maximum likelihood approach (Mattox et al. 1996) implemented in the *glike* utility, in which two model hypotheses were compared by their maximal likelihoods with respect to the observed photon distribution. The null hypothesis does not include the halo, the alternative hypothesis adds the halo to the list of sources of the null hypothesis.

The model includes 25 sources found within RoI from the 3FGL catalogue (Acero et al. 2015), the latest galactic interstellar emission model *gll\_iem\_v06\_rev1.fit*, and the isotropic spectral template *iso\_source\_v06.txt* $^2$ . Parameters (normalized flux and photon spectral index) of 16 out of 25 point-like and background sources were allowed to change $^3$ . We also included additional 69 point-like gamma-ray emitters from the 3FGL catalogue found between  $10^\circ$  and  $15^\circ$  from the RoI centre with their parameters held fixed.

The M31 galaxy itself was modelled as an extended source based on the IR observations (Miville-Deschênes & Lagache 2005) (100 $\mu$ m normalized IRIS map from the InfraRed Astronomical Satellite, IRAS) following the prescriptions of the Fermi LAT collaboration (Abdo et al. 2010).

Finally, extended halo spatial templates were inserted into the source model. We have used the simplest spatial models – uniformly bright circles of different radii (from

$0.1^\circ$  to  $5.0^\circ$  with  $0.1^\circ$  step). Of course, it is not a realistic model, because some decrease in surface brightness towards the outer halo regions can be expected. On the other hand, scarcity of the data used justifies this simple approach – a more sophisticated model would inevitably involve a larger number of parameters, which would make fitting much harder and would dilute any obtained significance as well.

The M31 galaxy and the halo spectra were described by a simple power-law model:

$$dN/dE \propto (E/E_0)^{-\Gamma} \quad (1)$$

The normalization and spectral index  $\Gamma$  were allowed to vary during the likelihood optimisation, while the energy scale  $E_0$  was fixed at 1 GeV.

The evidence of detection of gamma-ray signal from the halo was evaluated in terms of a likelihood ratio test statistic:

$$TS = -2 \ln \frac{L_{\max,0}}{L_{\max,1}} \quad (2)$$

where  $L_{\max,0}$  and  $L_{\max,1}$  are maximum likelihood values obtained from the observed data fit using null and alternative hypothesis, respectively. If the *alternative* hypothesis is true, then  $\sqrt{TS}$  is approximately equivalent to the source detection significance.

## 3 RESULTS

### 3.1 Uniform circle template

Firstly, we searched for diffuse gamma-ray emission from M31 galaxy itself. The galaxy was modelled in two different ways: as a point-like source or as an extended object (the IRAS template). The extended template for the M31 galaxy fits the data considerably better than the simple point-like source ( $TS_{\text{ext}} = 79$ ,  $TS_{\text{ps}} = 62.3$ ). The galaxy has a soft spectrum with photon index  $\Gamma = 2.40 \pm 0.12$  and the flux  $F = (2.6 \pm 0.4) \times 10^{-9}$  ph cm $^{-2}$  s $^{-1}$  in the 0.3-100 GeV energy range. The spectrum is even softer if the galaxy is modelled as a point-like source:  $\Gamma = 2.64 \pm 0.15$  with the photon flux  $F = (1.9 \pm 0.3) \times 10^{-9}$  ph cm $^{-2}$  s $^{-1}$ .

The results of fitting with additional halo component are presented in Fig. 1. The fit quality improvement can be easily seen. The highest statistical significance  $TS = 22$  was obtained for a halo with radius  $R_{\text{halo}} = 0.9^\circ$ , corresponding to a linear size of  $\sim 12$  kpc. The photon flux from the extended halo and the 0.3-100 GeV luminosity obtained from the fit are  $\sim (3.2 \pm 1.0) \times 10^{-9}$  cm $^{-2}$ s $^{-1}$  and  $(4.0 \pm 1.5) \times 10^{38}$  erg s $^{-1}$ , respectively, adopting the distance  $d = 780$  kpc. The spectral index is found to be rather soft:  $\Gamma = 2.30 \pm 0.12$ . A marginal improvement ( $TS \sim 8$ ) could be also achieved by adding a  $3^\circ$  halo ( $\sim 35$  kpc).

To exclude possible systematic and instrumental effects, which could affect our results, we have performed several additional tests:

(i) In order to check whether the size of the PSF, which for 68% containment is equal to  $\sim 2^\circ(4^\circ)$  for front- (back-) converted events at  $E = 300$  MeV, could result in an extended artefact, we performed Monte Carlo simulations. We have simulated events in the energy range 0.3–100 GeV for the relevant time span (71 months) and the RoI described above. The model included the following components: the

$^1$  <http://fermi.gsfc.nasa.gov/ssc/data/analysis/software/>

$^2$  <http://fermi.gsfc.nasa.gov/ssc/data/access/lat/BackgroundModels.html>

$^3$  The significance ( $TS$ ) of 9 out of 25 3FGL sources is less than 25, therefore their parameters were kept fixed.

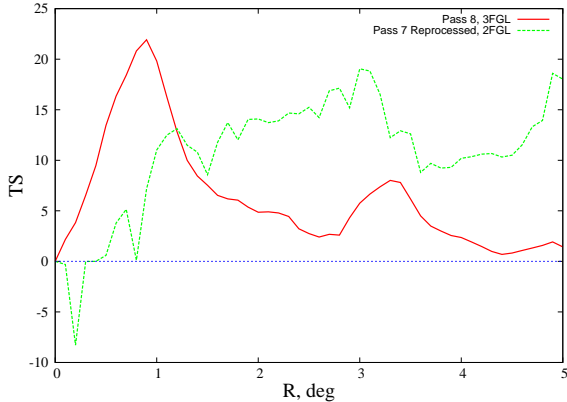


**Figure 1.**  $TS(R_{\text{halo}})$  curves: an earlier version (65 month of data, Pass7 Reprocessed events and 2FGL catalogue) is shown for comparison. The  $TS(R_{\text{halo}})$  curve is much smoother when the latest version of event reconstruction and the 3FGL source catalogue are used.

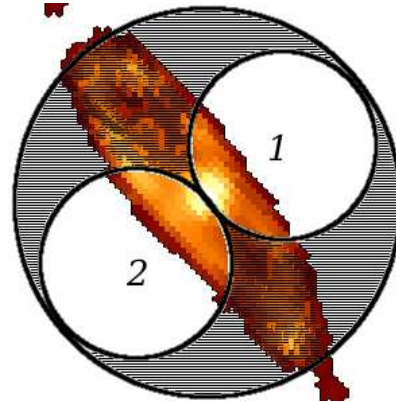


**Figure 3.** Model templates used for M31 halo fitting: IRAS template,  $0.9^\circ$  uniform circle, (1) and (2) –  $0.45^\circ$  bubbles perpendicular to the galactic plane, and region complementary to two bubbles (the shaded area).

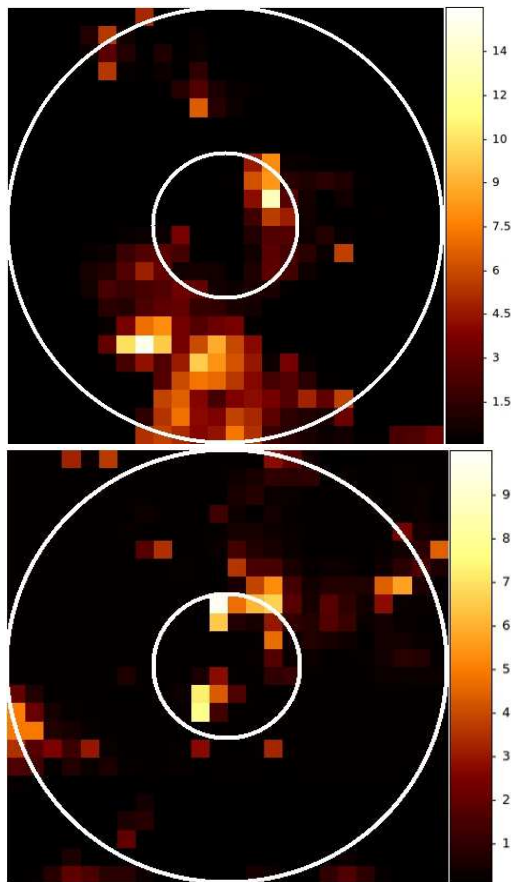


**Figure 2.** *Upper panel:* The grey-scale  $TS$  map with the IRAS template for the M31 disc. A complex extended structure around the galaxy is clearly seen.  $1^\circ$  and  $3^\circ$  white circles are shown for convenience. *Lower panel:* The grey-scale  $TS$  map of simulated data including  $0.9^\circ$  halo. A bright spot with  $TS \sim 10$  that emerged by chance is seen. There are no clear signs of any extended structure beyond the  $1^\circ$  radius.

galactic and isotropic background, point-like sources from the 3FGL catalogue, the M31 galaxy (using the IRAS  $100\mu\text{m}$  template) and an extended halo with  $R=0.9^\circ$  characterized by the power-law spectral index  $\Gamma = 2.2$  and photon flux  $F_{0.3-100\text{GeV}} = 1.5 \times 10^{-9} \text{ cm}^{-2}\text{s}^{-1}$ . Spectral parameters and photon fluxes for the point-like sources from the 3FGL were taken from the 3FGL catalogue, the recommended values were chosen for the isotropic and galactic background fluxes<sup>4</sup>. After that the simulated files were subjected to our standard analysis.

The resulting  $TS$  for the halo was found to be 17.1, the fitted power-law index was  $\Gamma = 1.96 \pm 0.09$  and the fitted photon flux  $F_{0.3-100\text{GeV}} = (1.46 \pm 0.23) \times 10^{-9} \text{ cm}^{-2}\text{s}^{-1}$ , the maximal  $TS$  was reached around  $R = 0.9^\circ$ . No  $TS$  increase was found in this analysis if no events from the halo were simulated. Therefore, we can conclude that the finite size of the PSF or leakage from an imperfect background treatment could produce spurious  $TS$  larger than 20.

(ii) In order to check whether the initial  $TS$  increase (Fig. 1) can be due to unidentified point-like sources not included into the 3FGL catalogue, we calculated the  $TS$  map using the *gttsmap* utility (see Fig. 2, upper panel). A  $TS$  excess at about  $0.9^\circ$  from the centre of the galaxy with the galactic coordinates ( $l = 120.58^\circ$ ,  $b = -21.17^\circ$ ) emerges that could be ascribed to FSRQ B3 0045+013. However, even after adding this source into our model, the  $TS$  of the uniform halo decreased only from 22 to 15 (the  $TS$  for this source was 11.2), thus the whole increase could not be attributed to this source alone. Alternatively, this  $TS$  excess could be produced by a small-scale inhomogeneity of the M31 halo. The plausibility of this scenario is also confirmed by the inspection of the  $TS$  maps of several simulated haloes – they are far from being smooth and uniform, but rather consist of several random knots that could have  $TS > 10$  (see Fig. 2, lower panel).

(iii) We also checked that the smallness of our RoI does not considerably affect our analysis: we have performed the

<sup>4</sup> <http://fermi.gsfc.nasa.gov/ssc/data/analysis/scitools/help/gtobssim.txt>

data analysis using a larger circle with  $15^\circ$  radius. The halo  $TS$  value remained essentially unchanged.

Several additional tests are presented in the Appendix.

### 3.2 Bubble template

Despite low statistics (600–700 photons), hints on the possible nature of the found extended emission could be inferred from its morphology. The first natural option is that the emission has hadronic origin – the cosmic rays are interacting with the diffuse medium, producing pions and, eventually, gamma-rays. In this case the emission brightness traces the concentration of targets, i.e., the gas density. Most of the gas mass of the M31 galaxy resides in a flat HI disc (see, e.g. (Cram et al. 1980; Robles-Valdez et al. 2014)) and the expected template should naturally have the shape of an ellipse with aspect ratio  $b/a = \cos i \sim 0.22$ , where  $a, b$  are the semi-major and semi-minor axes, respectively, and  $i = 77^\circ$  is the inclination angle. The results are presented in Fig. 4: addition of such a disc-like component does not improve the fit quality. In other words, IRAS+disc template describes the data much poorer than the IRAS+circle one. This implies that the hadronic origin of the extended halo due to the cosmic rays interactions with matter is strongly disfavoured.

The Fermi bubbles are almost circular regions of  $\sim 6$  kpc radius located above and below the Galactic centre, their total luminosity is equal to  $L_{\text{FB}} \sim 4 \times 10^{37}$  erg  $\text{s}^{-1}$ . They are believed to reflect past activity of the central region of the Galaxy, either from the central supermassive black hole (SMBH) or central star-formation burst. We decided to test whether a ‘FB-like’ morphology can fit the data better than the simple uniform disc template. First of all, we performed fits varying the bubble radius from 0.1 to 0.75 degrees. For each bubble radius, four different models were fitted (see Fig. 3). The results are shown in Fig. 5. There is a clear maximum for the FB 1+2 template with  $0.45 - 0.55^\circ$  radius of the bubbles (corresponding to the linear size 6-7.5 kpc), with  $TS = 28.2$ . The rest of the  $0.9^\circ$  circle (FB<sub>compl</sub> template) contributes very little. The parameters of the best-fit model are listed in Table 1. Additionally, we have searched for a possible ellipticity of the bubbles. The major semi-axes of both ellipses normal to the disc plane were fixed at  $a = 0.45^\circ$ , while the aspect ratio  $b/a$  was allowed to vary in the 0.1-0.9 range. Fig. 6 shows that although the signal is concentrated around the major semi-axes, it is not completely contained within this narrow jet-like region.

## 4 DISCUSSION AND CONCLUSIONS

Using almost 7 years of the Fermi-LAT observations, we performed search for an extended gamma-ray halo at energies above 300 MeV around the closest large spiral galaxy, M31. We find that the Fermi-LAT data suggest the presence of a spatially extended diffuse gamma-ray excess around M31. The best-fit morphology of the diffuse emission closely resembles the Fermi bubbles in the Milky Way. The best fit gave  $\sim 5.2\sigma$  significance for two  $0.45^\circ$  (6.5 kpc) bubbles with a photon flux of  $\sim (2.6 \pm 0.6) \times 10^{-9}$   $\text{cm}^{-2}\text{s}^{-1}$  and a luminosity of  $(3.2 \pm 0.6) \times 10^{38}$  erg  $\text{s}^{-1}$  in the energy range

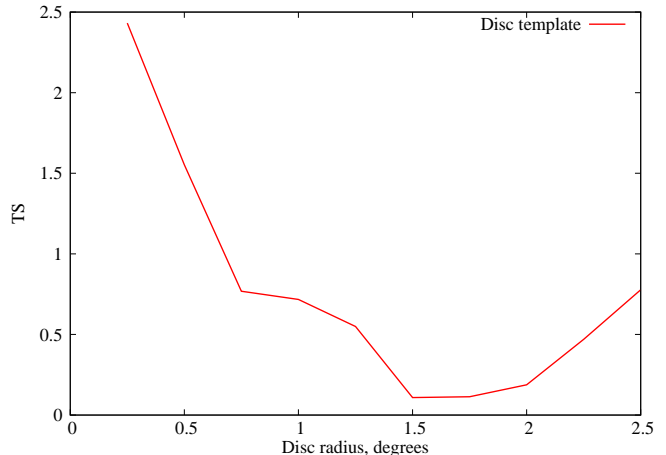


**Figure 4.**  $TS$  curve for an elliptic template with aspect ratio  $a/b = 0.22$ , representing addition of the HI disc-like emission. Inclusion of these templates does not improve the fit quality.

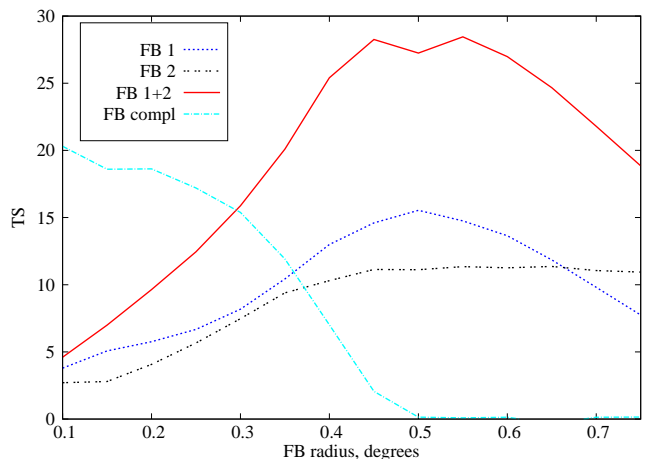


**Figure 5.**  $TS$  curves for different templates. Most of the signal comes from the region corresponding to the FB 1+2 template.

**Table 1.** Best-fit parameters for IRAS + different halo templates from Fig. 3. Column 1: model template, column 2:  $TS$  value, column 3: integral flux in the 0.3-100 GeV range, column 4: photon spectral index  $\Gamma$ . For comparison, best-fit parameters for uniform  $0.9^\circ$  template are also presented

model	$TS$	$F_{300}, 10^{-9}$ ( $\text{cm}^{-2} \text{s}^{-1}$ )	$\Gamma$
IRAS only	–	$2.9 \pm 0.4$	$2.4 \pm 0.1$
FB 1	14.6	$1.4 \pm 0.5$	$2.5 \pm 0.3$
FB 2	11.1	$0.72 \pm 0.35$	$2.0 \pm 0.2$
FB 1+2	28.2	$2.6 \pm 0.6$	$2.3 \pm 0.1$
FB <sub>compl</sub>	2.0	$1.1 \pm 0.9$	$2.5 \pm 0.4$
$0.9^\circ$ circle	22.0	$3.2 \pm 1.0$	$2.3 \pm 0.1$

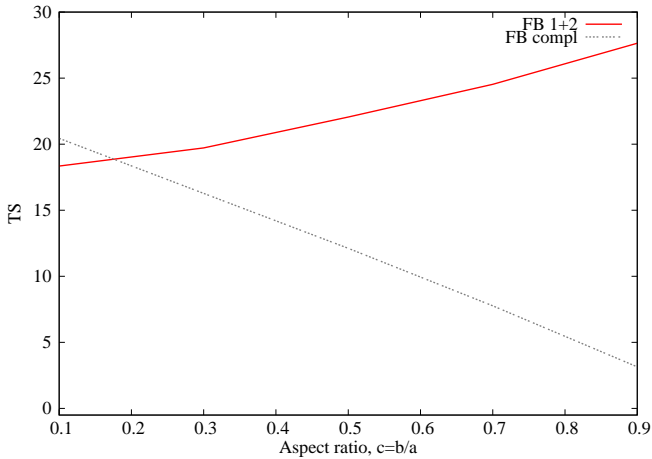


**Figure 6.**  $TS$  curve for elliptical FB templates with different aspect ratio  $b/a$ . The semi-major axis is fixed at  $a = 0.45^\circ$ . The complementary template is defined as above (see Fig. 3)

0.3–100 GeV. These parameters are fairly close to those of the Fermi bubbles in the Milky Way:  $r_{\text{FB}} \sim 6$  kpc, luminosity in the 0.1–500 GeV range  $4.4 \times 10^{37}$  erg  $\text{s}^{-1}$  with  $\Gamma = 1.9 \pm 0.2$  (Ackermann et al. 2014). The difference in the luminosity can be ascribed to the presence of a much more massive SMBH in the M31 centre. In view of this similarity, it would be interesting to search for a structure similar to the ‘WMAP haze’ at longer wavelengths (Finkbeiner 2004) around M31. The bubble-like morphology of the diffuse gamma-ray emission around M31 can hardly be explained by the standard DM-related scenarios. Past activity of the M31 galaxy might have been responsible for the complex structure of the  $TS$  excess at several degrees scale (see Fig. 2, upper panel).

Our findings suggest the possible ubiquity of the FB phenomenon in giant spiral galaxies related to their central activities. Future observations, including at energies  $> 100$  GeV (Bird et al. 2015; Smith et al. 2015) would certainly clarify this issue.

## ACKNOWLEDGEMENTS

The work was supported by the Grant of the President of Russian Federation MK-2138.2013.2, MK-4167.2015.2 and RFBR grant 14-02-00657. M.P. acknowledges the fellowship of the Dynasty foundation. The authors thank Drs. Dmitry Prokhorov, Igor Moskalenko, Ol’ga Sil’chenko and Anatoly Zasov for fruitful discussions. We also thank the anonymous referee for helpful suggestions. The analysis is based on data and software provided by the Fermi Science Support Center (FSSC). The numerical part of the work was done at the computer cluster of the Theoretical Division of INR RAS and cluster of the SAI MSU. This research has made use of NASA’s Astrophysics Data System.

## REFERENCES

- Abdo A. A., Ackermann M., Ajello M., Allafort A., Atwood W. B., Baldini L., Ballet J., Barbiellini G., Bastieri D., Bechtol K., Bellazzini R., Berenji B., Blandford R. D., et al. 2010, *A&A*, 523, L2
- Acero F., et al., 2015, *Astrophys. J. Suppl.*, 218, 23
- Ackermann M., et al., 2014, *Astrophys. J.*, 793, 64
- Bird R., et al., 2015, in *Proceedings of 34<sup>th</sup> International Cosmic Ray Conference, The Hague, 2015 VERITAS Observations Of M31 (The Andromeda Galaxy)*. *Proceedings of Science*, p. 851
- Blitz L., Robishaw T., 2000, *ApJ*, 541, 675
- Bregman J. N., Lloyd-Davies E. J., 2007, *ApJ*, 669, 990
- Cram T. R., Roberts M. S., Whitehurst R. N., 1980, *A&AS*, 40, 215
- De Paolis F., Gurzadyan V. G., Nucita A. A., Ingrassio G., Kashin A. L., Khachatryan H. G., Mirzoyan S., Poghossian E., Jetzer P., Qadir A., Vetrugno D., 2014, *A&A*, 565, L3
- De Paolis F., Ingrassio G., Jetzer P., Roncadelli M., 1999, *ApJ*, 510, L103
- Feldmann R., Hooper D., Gnedin N. Y., 2013, *ApJ*, 763, 21
- Finkbeiner D. P., 2004, *ApJ*, 614, 186
- Ford G. P., et al., 2013, *ApJ*, 769, 55
- Fukugita M., Peebles P. J. E., 2006, *ApJ*, 639, 590
- Kennicutt R. C., Evans N. J., 2012, *ARA&A*, 50, 531
- Lehner N., Howk J. C., Wakker B. P., 2015, *ApJ*, 804, 79
- Li J.-T., Li Z., Wang Q. D., Irwin J. A., Rossa J., 2008, *MNRAS*, 390, 59
- Mattox J. R., Bertsch D. L., Chiang J., Dingus B. L., Digel S. W., Esposito J. A., Fierro J. M., Hartman R. C., Hunter S. D., Kanbach G. e. a., 1996, *ApJ*, 461, 396
- Miller M. J., Bregman J. N., 2013, *ApJ*, 770, 118
- Miville-Deschênes M.-A., Lagache G., 2005, *ApJS*, 157, 302
- Putman M. E., Peek J. E. G., Joungh M. R., 2012, *ARA&A*, 50, 491
- Rao S. M., Sardane G., Turnshek D. A., Thilker D., Walterbos R., Vanden Berk D., York D. G., 2013, *MNRAS*, 432, 866
- Robles-Valdez F., Carigi L., Peimbert M., 2014, *Rev. Mex. Astron. Astrofis.*, 50, 271
- Smith A. J., et al., 2015, in *Proceedings of 34<sup>th</sup> International Cosmic Ray Conference, The Hague, 2015 HAWC: Design, Operation, Reconstruction and Analysis*. *Proceedings of Science*, p. 966
- Strong A. W., Moskalenko I. V., Ptuskin V. S., 2007, *Annual Review of Nuclear and Particle Science*, 57, 285
- Strong A. W., Porter T. A., Digel S. W., Jóhannesson G., Martin P., Moskalenko I. V., Murphy E. J., Orlando E., 2010, *ApJ*, 722, L58
- Su M., Slatyer T. R., Finkbeiner D. P., 2010, *ApJ*, 724, 1044
- Wang Q. D., Yao Y., Tripp T. M., Fang T.-T., Cui W., Nicastro F., Mathur S., Williams R. J., Song L., Croft R., 2005, *ApJ*, 635, 386
- Westmeier T., Braun R., Thilker D., 2005, *A&A*, 436, 101
- White S. D. M., Rees M. J., 1978, *MNRAS*, 183, 341

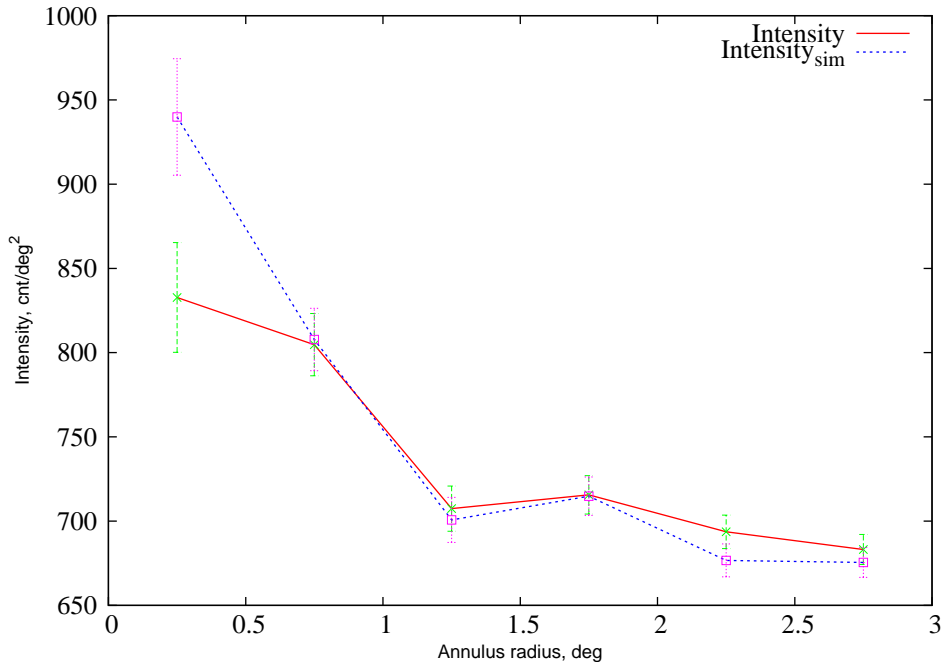


**Figure 7.** The data and simulations binned in  $0.5^\circ$  annuli. The simulations include backgrounds, point-like sources from the 3FGL catalogue, and IRAS+ $0.9^\circ$  halo with roughly equal contributions. The simulations well reproduce observations, being only slightly more concentrated towards the centre. This in turn may indicate that the IRAS (disc part) contribution to the data is subdominant.

## APPENDIX

Using *gtobssim* utility, we performed several tests in order to check for possible systematics.

(i) First of all, as an illustration, we show that the radial profile of the observed gamma-ray excess closely matches the one expected from the M31 galaxy (simulated by the IRAS template) and  $0.9^\circ$  halo, see Figure 7

(ii) We have also checked whether our method could be really sensitive to morphological features of the extended emission, since the possibility cannot be excluded that large  $TS$  can be produced by chance for, e.g., FB templates, which would erroneously lead us to wrong conclusions. To check this, we simulated six sets of events with different contribution from M31:

- No source;
- Point-like source with photon flux  $F_{0.3-100\text{GeV}} = 4.0 \times 10^{-9} \text{ cm}^{-2}\text{s}^{-1}$ . This flux corresponds to around 1100-1200 photons and slightly overestimates the actual excess. It is used only to make the possible difference more visible. This value was adopted in all simulations;
- IRAS template;
- IRAS template +  $0.9^\circ$  uniform halo with equal contributions to the total flux;
- $0.9^\circ$  uniform halo;
- 'Fermi bubble'-like structures with  $0.45^\circ$  radius.

These simulations were analyzed using different source models identical to ones used in the main text of the Letter:

- No source;
- Point-like source;
- IRAS template;
- IRAS +  $0.9^\circ$  uniform halo;
- IRAS + FB;
- IRAS +  $\text{FB}_{\text{compl}}$ .

The results are presented in Table 2.

(iii) In the case of  $0.9^\circ$  halo the total signal from the M31 region is dominated by the halo rather than the galaxy disc: the flux from the disc is found to be  $\sim 10\%$  of the total flux ( $\sim (3.3 \pm 1.0) \times 10^{-10} \text{ cm}^{-2}\text{s}^{-1}$ ). This fact suggests that the IR-based template cannot fully trace the gamma-ray emission, and this emission is far more extended than the template size. To find how the observed gamma-ray flux from the region is shared between the two components, we have simulated events in the energy range 0.3–100 GeV for the relevant time span (71 months) and the RoI described above. The model included the galactic and isotropic backgrounds, 16 point-like sources from the 3FGL catalogue, the M31 galaxy disc (taken in the form of the IRAS  $100\mu\text{m}$  template). Spectral parameters and photon fluxes for the point-like sources

**Table 2.** Results of the *gtlike* fit for different simulated sets:  $\Delta LLH$  for different models (with respect to the 'No source' model). Larger  $\Delta LLH$  indicate better models – our approach can distinguish different shapes of the extended emission, i.e., a uniform circle is better reconstructed with the uniform circle template, and the best reconstruction of a FB-like emission is achieved with the FB template.

Simulations	Model					
	No source	Point-like	IRAS	IRAS+Halo	IRAS+FB	IRAS+ FB <sub>compl</sub>
No source	0	2	3	-1	-1	-1
Point-like	0	<b>129</b>	108	104	105	104
IRAS	0	124	<b>204</b>	201	201	201
IRAS+Halo	0	102	172	<b>172</b>	172	169
Halo	0	81	131	<b>161</b>	152	142
FB	0	127	153	196	<b>220</b>	150

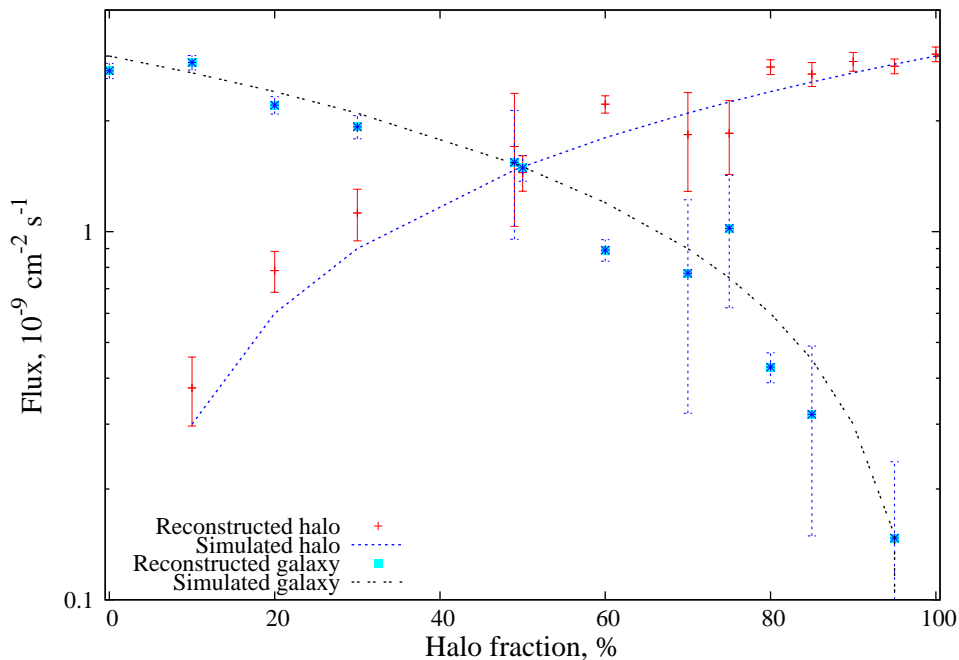


**Figure 8.** Comparison of the reconstructed and simulated fluxes from the disc and halo components for different halo fractions in the total flux.

were taken from the 3FGL catalogue. The recommended values were taken for the isotropic and galactic background fluxes (<http://fermi.gsfc.nasa.gov/ssc/data/analysis/scitools/help/gtobssim.txt>). We have fixed the total flux from the halo and disc components to a fiducial value  $3.0 \times 10^{-9} \text{ cm}^{-2} \text{ s}^{-1}$  and performed simulations, gradually changing the halo contribution from 0 to 100 %. The results are presented in Fig. 8. First of all, note that there is no leakage of the disc photons to the halo – when the fraction of the simulated halo photons is low, the results of the corresponding fit immediately show this. The same is true for the disc component as well. Clearly, this method can effectively separate the two components. The actual flux from the M31 galaxy disc is low,  $< 4 \times 10^{-10} \text{ cm}^{-2} \text{ s}^{-1}$ , therefore its luminosity in the 0.3-100 GeV energy range is rather modest:  $5 \times 10^{37} \text{ erg s}^{-1}$ . This value is several times as small as that of the Milky Way (Strong et al. 2010)<sup>5</sup>. This difference could be explained by low level of the star formation rate in M31, which is smaller than the corresponding Galactic rate by a factor of 4-5 (Kennicutt & Evans 2012; Ford et al. 2013). The lower star formation rate not only implies less energy in the form of cosmic rays that eventually produce the observed gamma-rays, but also means that the level of turbulence in the ISM of M31 is lower, which in turn leads to a rapid escape of CRs from the M31 disc region.

(iv) Finally, we show the best-fit results for all point-like sources within our RoI with parameters listed in Table 3.

<sup>5</sup> This luminosity also includes some contribution from the Milky Way halo, so the direct comparison is not straightforward

**Table 3.** Results of *gtlike* fit for the model that includes a  $0.9^\circ$  uniform halo. Benchmark values from the 3FGL catalogue are presented for comparison.

No.	Name of the source	3FGL normalization, $N_0 \times 10^{14}$	normalization with $0.9^\circ$ halo, $N_0 \times 10^{14}$	3FGL spectral index	Spectral index with halo	Distance, $^\circ$
1	3FGL J0039.1+4330	4.45	$3.60 \pm 0.57$	1.96	$2.06 \pm 0.12$	2.33
2	3FGL J0040.3+4049	0.042	$0.021 \pm 0.011$	1.13	$1.34 \pm 0.42$	0.64
3	3FGL J0048.0+3950	4.29	$6.15 \pm 0.52$	1.88	$1.90 \pm 0.06$	1.74
4	3FGL J0049.0+4224	0.86	$0.54 \pm 0.13$	1.76	$1.70 \pm 0.17$	1.63
5	3FGL J0102.3+4217	981	$973 \pm 97$	2.70	$2.86 \pm 0.10$	3.80
6	3FGL J0006.4+3825	612	$639 \pm 88$	2.62	$3.08 \pm 0.30$	7.50
7	3FGL J0023.5+4454	247	$164 \pm 23$	2.57	$2.60 \pm 0.14$	5.05
8	3FGL J0043.8+3425	81.4	$134 \pm 5$	2.04	$1.96 \pm 0.03$	6.84
9	3FGL J0105.3+3928	59	$62.3 \pm 6$	2.32	$2.17 \pm 0.08$	4.66
10	3FGL J0008.0+4713	56.8	$54.3 \pm 2$	2.02	$2.00 \pm 0.03$	5.68
11	3FGL J0058.3+3315	116	$215 \pm 147$	2.41	$1.39 \pm 0.62$	8.58
12	3FGL J0102.8+4840	245	$99 \pm 99$	1.77(PLEC)	$0.50 \pm 0.67$	8.20
13	3FGL J0106.5+4855	312	$410 \pm 286$	1.21(PLEC)	$1.45 \pm 0.50$	8.72
14	3FGL J0128.5+4430	60	$3.5 \pm 11 (TS \sim 2)$	2.33	–	8.98
15	3FGL J2356.0+4037	1.5	Removed ( $TS < 0$ )	1.72	–	8.82
16	3FGL J2358.5+3827	4.8	$361 \pm 200$	2.07	$1.19 \pm 0.30$	8.93